Field-Theoretic Renormalization Group Methods for a Two-Species Reaction-Diffusion Process with Lévy Flights

Troy Tsubota,[1] Adele Basturk,[1] and Nicholas Lawson[1]

[1] *Department of Physics, Harvard University, Cambridge, MA 02138, United States*

(Dated: May 15, 2026)

We study the two-species annihilation reaction $A + B \to 0$ with standard diffusion and with long-ranged Lévy flights described by the parameter σ, seeking the asymptotic decay rate of the minority species. We systematically present the procedure, from the Doi-Peliti formalism through the subsequent renormalization group analysis needed to find corrections to scaling below the upper critical dimension. The upper critical dimension shifts from $d_c = 2$ in standard diffusion to $d_c = \sigma$ with Lévy flights. Although this shift is understood for the single-species reaction, the asymptotics of the two-species reaction are more complex: the initial density difference between the two species can dramatically alter the dynamics. Finally, we support our study with numerical simulations.

I. INTRODUCTION

The renormalization group (RG) is the central tool for understanding the effects of fluctuations in many-body systems. The RG was first developed for systems in thermal equilibrium, where the Boltzmann distribution allows for direct calculations. However, many driven and relaxational systems also exhibit critical behavior that can be understood using RG methods. Although we cannot write probability distributions for a large class of non-equilibrium steady states, systems described by stochastic partial differential equations are amenable to RG analysis through a field-theoretic representation [1].

In this paper, we apply field-theoretic RG methods for reaction-diffusion problems, as reviewed in Ref. [1], to the two-species annihilation reaction $A + B \to 0$. We first treat the case that A and B both undergo standard diffusion. Next, we allow A to undergo Lévy flights, or long-range hops with a heavy-tailed power-law distribution, motivated by foraging and search processes [2–4].

The reaction $A + A \to 0$ with Lévy flights [5] and the reaction $A + B \to 0$ with standard diffusion [6] have previously been studied [1, 7]. Fewer works have combined multi-species reactions with Lévy flights [8–10], and the complex reactions studied in these works limit clarity. Further, even $A + B \to 0$ with standard diffusion has scattered results not presented in a unified manner.

Here, we systematically present the field-theoretic RG method for the reaction $A + B \to 0$ with and without Lévy flights. We first review the Doi-Peliti formalism for mapping an arbitrary chemical reaction to a bosonic field theory [11, 12]. Then, we calculate the asymptotic decay statistics of the minority species' densities for the reaction, both in the mean-field limit and with RG corrections. In the case of Lévy flights, we show that the RG analysis is altered in the expected way, with the upper critical dimension modified to $d_c = \sigma$ with $\sigma < 2$ describing the magnitude of the superdiffusivity. Finally, we compare our theoretical results to numerical simulations. The simulations also allow us to study the scaling of the reaction and depletion zones between segregated A and B domains, offering directions for future work.

II. DOI-PELITI FIELD THEORY

Here we review the Doi-Peliti formalism for mapping a chemical reaction to a field theory. Consider two species of particles, A and B, with z neighbors on a lattice with spacing h. A Lévy flight is a random walk in which step sizes are drawn from a probability distribution of the form $P(r) \sim r^{-(d+\sigma)}$, where $\sigma < 2$. In order to treat the general case, we let A particles perform a continuous-time Lévy flight on a lattice, where particles at site i can jump to any site j with a rate that decays with the Lévy power law in the dimensionless distance $r_{ij} \equiv \sqrt{\sum_{k=1}^{d} (i_k - j_k)^2}$.

B particles perform a continuous time random walk, hopping to a neighboring site at a uniform rate $D_B h^{-2}$ [1]. When more than one particle occupies the same site, they annihilate at a fixed reaction rate λ. The probability distribution $P(\{n\}, \{m\}, t)$ characterizes the state of the system at time t, where $\{n\} = (n_1, n_2, \cdots)$ and $\{m\} = (m_1, m_2, \cdots)$ specify the configuration of A and B particles, respectively. The master equation for the time evolution of the configuration probability due to hops can be written as

$$
\begin{aligned}
&\partial_t P(\{n\}, \{m\}, t) = \\
&\quad D_A h^{-\sigma} \sum_{i \neq j} \frac{1}{r_{ij}^{d+\sigma}} \\
&\times \Big[(n_i{+}1)\, P(\{m\}, \ldots, n_i{+}1, n_j{-}1, \ldots, t) \\
&\quad - n_i\, P(\{n\}, \{m\}, t) \\
&\quad + (n_j{+}1)\, P(\{m\}, \ldots, n_i{-}1, n_j{+}1, \ldots, t) \\
&\quad - n_j\, P(\{n\}, \{m\}, t) \Big] \\
&\quad + D_B h^{-2} \sum_{\langle ij \rangle} \Big[(m_i{+}1)\, P(\{n\}, \ldots, m_i{+}1, m_j{-}1, \ldots, t) \\
&\quad - m_i\, P(\{n\}, \{m\}, t) \\
&\quad + (m_j{+}1)\, P(\{n\}, \ldots, m_i{-}1, m_j{+}1, \ldots, t) \\
&\quad - m_j\, P(\{n\}, \{m\}, t) \Big].
\end{aligned}
\tag{1}
$$

The summation for A particles extends over all pairs in the lattice, while the summation for B particles extends only over pairs of nearest-neighbor sites. Within the sum, hops from i to j and j to i are both considered. We define this as the travel term. Adding the annihilation reaction $A + B \to 0$, the full master equation assumes the form

$$\begin{aligned}\partial_t P(\{n\},\{m\},t) = &\ \text{(travel term)} \\ &+ \lambda \sum_i \Big[(m_i+1)(n_i+1)P(\ldots,m_1+1,\ldots,n_1+1,\ldots,t) \\ &- m_i n_i P(\{n\},\{m\},t)\Big]\end{aligned} \tag{2}$$

Next, we use the Doi-Peliti formalism to map the classical probability distribution described by the master equation onto a quantized bosonic field. In 1976, Doi showed that stochastic reaction-diffusion systems can be described by quantized ladder operators similar to those familiar from quantum mechanics [11]. The algebraic structure of second quantization naturally captures the property that site occupation number is always a positive integer. For each lattice sites i and j, the bosonic commutation relations for the creation and annihilation operators for species A and B are given by

$$[\hat{a}_i, \hat{a}_j^\dagger] = [\hat{b}_i, \hat{b}_j^\dagger] = \delta_{ij} \tag{3}$$

$$[\hat{a}_i, \hat{a}_j] = [\hat{b}_i, \hat{b}_j] = [\hat{a}_i^\dagger, \hat{a}_j^\dagger] = [\hat{b}_i^\dagger, \hat{b}_j^\dagger] = 0. \tag{4}$$

Denote the empty lattice as $|0\rangle$ such that $a_i |0\rangle = b_i |0\rangle = 0$ for all i. Each site i is associated with a state vector $|n_i\rangle = (\hat{a_i}^\dagger)^{n_i} |0\rangle$, $|m_i\rangle = (\hat{b_i}^\dagger)^{m_i} |0\rangle$, following the normalization convention: $\hat{a}_i |n_i\rangle = n_i |n_i - 1\rangle$, $\hat{a}_i^\dagger |n_i\rangle = |n_i + 1\rangle$, and analogously for the corresponding b operators. Using the on-site vectors to denote the state of the entire system at time t,

$$|\phi(t)\rangle = \sum_{\{n\}} P(\{n\},\{m\},t) \prod_i (\hat{a}_i^\dagger)^{n_i} (\hat{b}_i^\dagger)^{m_i} |0\rangle \tag{5}$$

we obtain the imaginary time evolution equation

$$-\partial_t |\phi(t)\rangle = \hat{H} |\phi(t)\rangle \tag{6}$$

where the non-Hermitian Hamiltonian is

$$\begin{aligned}\hat{H} = &\ D_A h^{-\sigma} \sum_{i \neq j} \frac{(\hat{a}_i^\dagger - \hat{a}_j^\dagger)(\hat{a}_i - \hat{a}_j)}{r_{ij}^{d+\sigma}} \\ &+ D_B h^{-2} \sum_{\langle ij \rangle} (\hat{b}_i^\dagger - \hat{b}_j^\dagger)(\hat{b}_i - \hat{b}_j) \\ &- \lambda \sum_i \Big[1 - \hat{a}_i^\dagger \hat{b}_i^\dagger\Big] \hat{a}_i \hat{b}_i\end{aligned} \tag{7}$$

In the Lévy term, $\hat{a_j}^\dagger \hat{a}_i - \hat{a_i}^\dagger \hat{a}_i$ represents a hop from i to j; the number operator $\hat{a}_i^\dagger \hat{a}_i$ does not change the state. The term $\hat{a}_i^\dagger \hat{a}_j - \hat{a}_j^\dagger \hat{a}_j$ represents the equivalent process from j to i. The same is true for the diffusive term with the b operators. Note that the operator structure of the effective Hamiltonian reproduces the eigenvalue coefficients and state dependencies in Eq. (1). In the reaction term, the term $\hat{a}_i \hat{b}_i$ describes the annihilation of one A particle and one B particle at site i. The term $\hat{a}_i^\dagger \hat{b}_i^\dagger \hat{a}_i \hat{b}_i$ represents the number of particle pairs available to react, with eigenvalue $m_i n_i$ equivalent to the coefficient of the loss term in the master equation.

To define a field theory, let $\hat{a}_i, \hat{a}_i^\dagger \to \phi_i, \phi_i^*$, where ϕ is complex. Having changed variables to ϕ and ϕ^*, which commute, we must correctly map $\hat{H}(\hat{a}, \hat{a}^\dagger, \hat{b}, \hat{b}^\dagger) \to \hat{H}(\phi_a, \phi_a^*, \phi_b, \phi_b^*)$. We can do this since the coherent states $|\phi\rangle$ are eigenstates of the lowering operator $\hat{a}$ with eigenvalue ϕ. Thus, the expectation value of the Hamiltonian in the coherent state basis only depends on ϕ and its conjugate field.

The coherent states for species A and B at site i are defined by

$$|\phi_{a,i}\rangle = e^{-|\phi_{a,i}|^2/2 + \phi_{a,i}\hat{a}_i^\dagger} |0\rangle , \tag{8}$$

$$|\phi_{b,i}\rangle = e^{-|\phi_{b,i}|^2/2 + \phi_{b,i}\hat{b}_i^\dagger} |0\rangle , \tag{9}$$

with overlaps between two different field values $\phi_{a,i}$ and $\phi'_{a,i}$ at the same site,

$$\langle \phi_{a,i} | \phi'_{a,i} \rangle = e^{-|\phi_{a,i}|^2/2 - |\phi'_{a,i}|^2/2 + \phi^*_{a,i}\phi'_{a,i}}, \tag{10}$$

$$\langle \phi_{b,i} | \phi'_{b,i} \rangle = e^{-|\phi_{b,i}|^2/2 - |\phi'_{b,i}|^2/2 + \phi^*_{b,i}\phi'_{b,i}}. \tag{11}$$

Since the coherent-state basis is overcomplete, the identity for each species is

$$1 = \int \frac{d^2\phi_{a,i}}{\pi} \, |\phi_{a,i}\rangle \langle \phi_{a,i}| \tag{12}$$

$$= \int \frac{d^2\phi_{b,i}}{\pi} \, |\phi_{b,i}\rangle \langle \phi_{b,i}| . \tag{13}$$

To generalize to the full lattice, define $\{\phi_a\} = (\phi_{a,1}, \phi_{a,2}, \ldots)$ and $\{\phi_b\} = (\phi_{b,1}, \phi_{b,2}, \ldots)$ as the sets of coherent-state eigenvalues for species A and B across all sites, with the joint state vector

$$|\{\phi_a\}, \{\phi_b\}\rangle = \bigotimes_i |\phi_{a,i}\rangle \otimes |\phi_{b,i}\rangle . \tag{14}$$

The final normalization is given by

$$1 = \int \prod_i \frac{d^2\phi_{a,i}}{\pi} \frac{d^2\phi_{b,i}}{\pi} \, |\{\phi_a\}, \{\phi_b\}\rangle \langle \{\phi_a\}, \{\phi_b\}| . \tag{15}$$

The coherent-state basis requires that $\hat{H}$ is normal ordered, i.e. that all $\hat{a}^\dagger$ are to the left of all $\hat{a}$. As such, the normal-ordered operator $\hat{H}(\hat{a}^\dagger, \hat{a})$ can be recast as

$$\langle\{\phi_a\},\{\phi_b\}|\,\hat{H}(\hat{a}^\dagger,\hat{a},\hat{b}^\dagger,\hat{b})\,|\{\phi_a\},\{\phi_b\}\rangle = H(\{\phi_a^*\},\{\phi_b^*\},\{\phi_a\},\{\phi_b\}) \tag{16}$$

The diffusion terms $(\hat{a}_i^\dagger-\hat{a}_j^\dagger)(\hat{a}_i-\hat{a}_j)$, $(\hat{b}_i^\dagger-\hat{b}_j^\dagger)(\hat{b}_i-\hat{b}_j)$ and the reaction term $-\lambda\sum_i\left[1-\hat{a}_i^\dagger\hat{b}_i^\dagger\right]\hat{a}_i\hat{b}_i$ are already normal-ordered. As before, one simply replaces $\hat{a}_i,\hat{b}_i\to\phi_{a,i},\phi_{b,i}$ and $\hat{a}_i^\dagger,\hat{b}_i^\dagger\to\phi_{a,i}^*,\phi_{b,i}^*$, the eigenvalues of the raising and lowering operators acting on the coherent states. Therefore, we can rewrite the Hamiltonian as

$$\begin{aligned}&\hat{H}(\{\phi_a^*\},\{\phi_b^*\},\{\phi_a\},\{\phi_b\}) = \\ &D_A h^{-\sigma}\sum_{i\neq j}\frac{(\phi_{a,i}^*-\phi_{a,j}^*)(\phi_{a,i}-\phi_{a,j})}{r_{ij}^{d+\sigma}} \\ &+D_B h^{-2}\sum_{\langle ij\rangle}(\phi_{b,i}^*-\phi_{b,j}^*)(\phi_{b,i}-\phi_{b,j}) \\ &-\lambda\sum_i(1-\phi_{a,i}^*\phi_{b,i}^*)\phi_{a,i}\phi_{b,i}\end{aligned} \tag{17}$$

We can relate the Hamiltonian to the action $S[\phi,\phi^*]$ through the following path integral

$$1=\langle\mathcal{P}|\;e^{-\hat{H}t_f}\;|\phi(0)\rangle=\int\mathcal{D}\phi\,\mathcal{D}\phi^*\;e^{-S[\phi,\phi^*]}. \tag{18}$$

where, given that the Hamiltonian resulting from the master equation is non-Hermitian, we define a projection state $\langle\mathcal{P}|$. $\langle\mathcal{P}|$ has the properties $\langle\mathcal{P}|\hat{a}_i^\dagger=\langle\mathcal{P}|$ and $\langle\mathcal{P}|0\rangle=1$ such that $\langle\mathcal{P}|=\langle 0|e^{\sum_i\hat{a}_i}$. The ensemble average for an operator $\hat{\mathcal{O}}$ takes the form $\bar{\mathcal{O}}(t)=\langle\mathcal{P}|\hat{\mathcal{O}}|\phi(t)\rangle$. Unitarity is enforced through

$$\langle\mathcal{P}|\phi(t)\rangle=\langle\mathcal{P}|e^{-\hat{H}t}|\phi(0)\rangle=1. \tag{19}$$

Given the quantized theory derived from the master equation, we next obtain a field theory and a corresponding action using a path integral. We discretize time, such that $\Delta t=t/N$, and perform a Trotter decomposition: $e^{-\hat{H}t}\,|\phi(0)\rangle=\lim_{\Delta t\to 0}e^{(-\hat{H}\Delta t)^{t/\Delta t}}\,|\phi(0)\rangle$.

Inserting the Trotter decomposition with N terms $e^{-\hat{H}t_f}=e^{-\hat{H}\Delta t}\,e^{-\hat{H}\Delta t}\cdots e^{-\hat{H}\Delta t}$ and using the identity in Eq. (12), a single slice from k to $k+1$ of the decomposed Hamiltonian matrix element factorizes as

$$\langle\{\phi_{k+1}\}|\;e^{-\hat{H}\Delta t}\;|\{\phi_k\}\rangle=\langle\{\phi_{k+1}\}|\{\phi_k\}\rangle\;e^{-\Delta t\,H(\phi_{k+1}^*,\phi_k)}, \tag{20}$$

For the lattice sites i we can write the coherent state overlap following from Eq. (10) as

$$\langle\{\phi_{k+1}\}|\{\phi_k\}\rangle = \exp\left[\sum_i\left(\phi_{k+1,i}^*\phi_{k,i}-\tfrac{1}{2}|\phi_{k+1,i}|^2-\tfrac{1}{2}|\phi_{k,i}|^2\right)\right] \tag{21}$$

Therefore,

$$\begin{aligned}&\langle\{\phi_{k+1}\}|\;e^{-\hat{H}\Delta t}\;|\{\phi_k\}\rangle \\ &=\exp\sum_i\left(\phi_{k+1,i}^*\phi_{k,i}-\tfrac{1}{2}|\phi_{k+1,i}|^2-\tfrac{1}{2}|\phi_{k,i}|^2\right) \\ &-\Delta t\,H(\phi_{k+1}^*,\phi_k)\end{aligned} \tag{22}$$

In the limit that $\Delta t\to 0$ and $N\Delta t=t_f$, where t_f is a fixed constant, the above expression becomes

$$1=\int\mathcal{D}\phi_{a,b}^*\,\mathcal{D}\phi_{a,b}\;\exp\{-\int_0^{t_f}dt\left(\phi_a^*\partial_t\phi_a+\phi_b^*\partial_t\phi_b+H(\phi_a^*,\phi_a,\phi_b^*,\phi_b)\right)\} \tag{23}$$

Taking the continuum limit of the lattice, the index i becomes a coordinate x, $\sum_i\to h^{-d}\int d^dx$, and lattice variables become a continuum field $\phi_i(t)\to\phi(x,t)$. The two diffusion terms become

$$\sum_{\langle ij\rangle}(\phi_i^*-\phi_j^*)(\phi_i-\phi_j)\to\;h^{2-d}\int d^dx\,\nabla\phi^*\cdot\nabla\phi \tag{24}$$

$$=-h^{2-d}\int d^dx\,\phi^*\nabla^2\phi, \tag{25}$$

For Lévy flights, we follow the same procedure, using a symmetrization trick

$$\begin{aligned}&\sum_{i\neq j}\frac{(\phi_i^*-\phi_j^*)(\phi_i-\phi_j)}{|i-j|^{d+\sigma}} \\ &\longrightarrow h^{\sigma-d}\iint d^dx\,d^dy\,\frac{[\phi^*(x)-\phi^*(y)][\phi(x)-\phi(y)]}{r_{xy}^{d+\sigma}} \\ &=2\,h^{\sigma-d}\int d^dx\,\phi^*(x)\int d^dy\,\frac{\phi(x)-\phi(y)}{r_{xy}^{d+\sigma}} \\ &=2h^{\sigma-d}\int d^dx\,\phi^*(x)\,(-\nabla^2)^{\sigma/2}\phi(x) \\ &\propto -h^{\sigma-d}\int d^dx\,\phi^*\,\nabla^\sigma\phi.\end{aligned} \tag{26, 27}$$

Finally, the reaction term in the continuum limit is given by

$$-\lambda\sum_i\left(1-\phi_{a,i}^*\phi_{b,i}^*\right)\phi_{a,i}\phi_{a,i} \tag{28}$$

$$\to-\lambda\,h^{-d}\int d^dx\left(1-\phi_a^*\,\phi_b^*\right)\phi_a\,\phi_b \tag{29}$$

Therefore, the full action is given by

$$\tilde{S}[\phi_a^*,\phi_a,\phi_b^*,\phi_b] = \int d^dx\Big[-\phi_a^*(t_f) - \phi_b^*(t_f) + \int_0^{t_f} dt\,\Big(\phi_a^*\left(\partial_t - D_A\nabla^\sigma\right)\phi_a + \phi_b^*\left(\partial_t - D_B\nabla^2\right)\phi_b - \lambda_0\left(1-\phi_a^*\,\phi_b^*\right)\phi_a\,\phi_b\Big) - n_0\,\phi_a^* a(0) - m_0\,\phi_b^*(0)\Big], \tag{30}$$

where $\lambda_0 = \lambda h^d$. Probability conservation forces $H(\phi^*=1,\phi)=0$. Taking the time derivative,

$$0 = \partial_t \langle\mathcal{P}|\phi(t)\rangle = \langle\mathcal{P}|\,\partial_t\,|\phi(t)\rangle = -\langle\mathcal{P}|\,\hat{H}\,|\phi(t)\rangle\,. \tag{31}$$

Since this must hold for any initial state,

$$\langle\mathcal{P}|\,\hat{H} = 0 \tag{32}$$

$$\langle\mathcal{P}|\,\hat{H}\,|\{\phi\}\rangle = H(\phi^*=1,\phi)\;\langle\mathcal{P}|\{\phi\}\rangle = 0. \tag{33}$$

The shifted variable $\phi^* = 1+\bar{\phi}$ is more natural, such that $\bar{\phi}=0$ is now the zero-fluctuation point and $\bar{\phi}$ denotes deviations. The new field $\bar{\phi}$ plays the role of a response field, and a conjugate to the noise of the stochastic dynamics in the system. As a result, we can remove the constant offset terms $-\phi^*(t_f) = -1-\bar{\phi}(t_f)$ and $-n_0\phi^*(0) = -n_0 - n_0\bar{\phi}(0)$, leaving only $-n_0\bar{\phi}(0)$ and $-m_0\bar{\phi}(0)$. The final result for the action, relabeling $\phi_a\to a$ and $\phi_b\to b$, is

$$S[\bar{a},a,\bar{b},b] = \int d^dx\Big[\int_0^{t_f} dt\Big(\bar{a}\left(\partial_t - D_A\nabla^\sigma\right)a + \bar{b}\left(\partial_t - D_B\nabla^2\right)b + \lambda_0\left(\bar{a}+\bar{b}+\bar{a}\bar{b}\right)ab\Big) - n_0\bar{a}(0) - m_0\bar{b}(0)\Big]. \tag{34}$$

III. MEAN FIELD THEORY

A mean-field description of the above process can be written as the kinetic rate equations:

$$\frac{da}{dt} = \frac{db}{dt} = -\lambda_0 ab. \tag{35}$$

This is a form of the *law of mass action* in chemistry. In the case of unequal initial densities $a_0 < b_0$, in long times it is easy to see that $a(t)\sim a_0 e^{-\lambda_0 t}$.

In the case of equal initial densities, a "slow mode" arises due to initial fluctuations in the conserved difference field $c = a-b$. To see this, it is more informative to include spatial variation and examine the two-field partial differential equations

$$\frac{\partial a(x,t)}{\partial t} = D_A\nabla^\sigma a - \lambda_0 ab \tag{36}$$

$$\frac{\partial b(x,t)}{\partial t} = D_B\nabla^2 b - \lambda_0 ab \tag{37}$$

where the fractional Laplacian $\nabla^\sigma = (\nabla^2)^{\sigma/2}$ is defined by its action in Fourier space

$$\nabla^\sigma e^{ik\cdot x} = (\nabla^2)^{\sigma/2}e^{ik\cdot x} = -|k|^\sigma e^{ik\cdot x}. \tag{38}$$

This is distinct from the Langevin equation description because it does not include noise (i.e. fluctuations). The connection between the Langevin description and Doi-Peliti field theory is subtle; see Ref. [13] for details.

We now follow Täuber et al. [7]: first consider $D_A = D_B$ and $\sigma = 2$. The density difference has dynamics

$$\frac{\partial c}{\partial t} = D\nabla^2 c. \tag{39}$$

This is the heat equation, with Green's function

$$G(x,t) = \frac{1}{(4\pi Dt)^{d/2}}\exp\left(-\frac{|x|^2}{4Dt}\right) \tag{40}$$

for $t>0$. The solution is then

$$c(x,t) = \int d^dx' G(x-x',t)\,c(x',0). \tag{41}$$

The Poisson distribution for each species over initial conditions implies $\overline{c(x,0)c(x',0)} = 2a_0\,\delta(x-x')$. Thus,

$$\overline{c(x,t)^2} = 2a_0\int d^dx' G(x-x',t)^2 = \frac{2a_0}{(8\pi Dt)^{d/2}} \tag{42}$$

and the local density excess is

$$\left[\overline{c(x,t)^2}\right]^{1/2} = \frac{\sqrt{2a_0}}{(8\pi Dt)^{d/4}}. \tag{43}$$

Thus, the density decays as $a(t)\sim(Dt)^{-d/4}$.

We now examine the new case with Lévy flights. We begin with

$$\frac{\partial c}{\partial t} = D\nabla^\sigma c. \tag{44}$$

We could in principle follow a similar argument as above, but we only need to extract the scaling. We argue that the Green's function here has scaling form

$$G_\sigma(x,t) = \frac{1}{(Dt)^{d/\sigma}} f\left(\frac{|x|}{(Dt)^{1/\sigma}}\right). \tag{45}$$

The argument is dimensionless based on dimensional analysis of Eq. (44), and the prefactor enforces

$\int d^d x\, G_\sigma(x,t) = \text{const.}$, i.e. conservation of c. Then,

$$\overline{c(x,t)^2} \sim \int d^d x' G_\sigma(x-x',t)^2 \tag{46}$$

$$\sim \frac{1}{(Dt)^{d/2\sigma}} \int d^d x' f^2\left(\frac{|x'|}{(Dt)^{1/\sigma}}\right) \tag{47}$$

$$\sim \frac{1}{(Dt)^{d/\sigma}} \int d^d \xi\, f^2(|\xi|). \tag{48}$$

Thus, $\left[\overline{c(x,t)^2}\right]^{1/2} \sim (Dt)^{-d/2\sigma}$.

Here, we made the simplification that both A and B undergo Lévy flights with the same diffusion constant $D = D_A = D_B$. We find that this simplification to be acceptable based on the analysis below.

Because of the dimension dependence up through $d = 4$ (or $d = 2\sigma$), some argue that this should be the upper critical dimension [1]. However, we take the upper critical dimension to be the dimension below which fluctuations are relevant. For standard reaction-diffusion problems, this is $d_c = 2$ [1]. Below, for Lévy flights, we find that $d_c = \sigma$.

IV. RG ANALYSIS OF $A + B \to 0$

Here we extend the renormalization group techniques presented by Täuber et al. to study the two-species annihilation reaction $A + B \to 0$ at rate λ_0. We initially consider the case that A and B both undergo standard diffusion, then generalize to the case that one, or both, species undergo Lévy flights.

A. $A + B \to 0$: standard diffusion

We write the Doi-Peliti action (34) for standard diffusion of both particles (i.e. $\sigma = 2$) as

$$S[a,\bar{a},b,\bar{b}] = \int dt d^d x [\bar{a}\left(\partial_t - D_A\nabla^2\right) a + \bar{b}\left(\partial_t - D_B\nabla^2\right) b + \lambda_0\left(\bar{a} + \bar{b} + \bar{a}\bar{b}\right) ab] - \int d^d x [\bar{a}(x,0)a_0 - \bar{b}(x,0)b_0] \tag{49}$$

We identify the Gaussian part of the action:

$$S_0 = \int d^d x dt \left[\bar{a}\left(\partial_t - D_A\nabla^2\right) a + \bar{b}\left(\partial_t - D_B\nabla^2\right) b\right] \tag{50}$$

After Fourier transforming, we can read off the bare propagators:

$$G_\alpha(\omega,p) = \frac{1}{-i\omega + D_\alpha p^2} \tag{51}$$

where $\alpha \in \{A, B\}$.

The first step is to identify the primitively divergent diagrams. As Täuber et al. note, all vertices in the action have two incoming lines, such that it is impossible to construct a loop diagram that renormalizes the propagator (for example, an incoming a and an outgoing $\bar{a}$). Thus, in this simple example, the bare diffusion constant is not renormalized. By a similar reasoning, there is no wavefunction renormalization for the fields either. Thus, all that remains is to calculate the renormalization of the bare reaction rate λ_0.

The core object is the vertex function $\tilde{\Gamma}$, i.e. the connected, amputated, one-particle irreducible Green's function. At the tree level, by construction, we have $\tilde{\Gamma}_{\text{tree}} = \lambda_0$, the bare reaction rate. The goal is to use a perturbative expansion in the nonlinear action to compute the full renormalized vertex function.

The relevant one-loop diagram is shown below, following the convention in the reaction-diffusion literature that time flows from right to left:

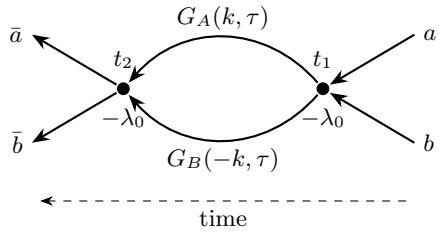

Since the diagrams will be dominated by a UV divergence of the loop momenta, it suffices to evaluate the diagrams at zero external momenta. A simple power-counting argument shows that derivatives of the vertex function with respect to the external momenta, as would appear in an expansion in small external momenta, are less badly divergent in the UV, justifying our setting the external momenta to zero. Momentum conservation requires that one propagator in the loop carry momentum k, the other $-k$, and we must integrate over k. By the usual perturbative expansion, each vertex contributes a factor of $-\lambda_0$. Thus the amputated one-loop correction to the vertex function takes the form

$$\delta\tilde{\Gamma}_1(t_2 - t_1) = (-\lambda_0)^2 \int \frac{d^d k}{(2\pi)^d} G_A(k, t_2 - t_1) G_B(-k, t_2 - t_1) \tag{52}$$

where the propagators in (p,t) coordinates can be obtained by the partial inverse Fourier transform to give (with a slight abuse of notation)

$$G_\alpha(p,t) = \Theta(t) e^{-D_\alpha p^2 t} \tag{53}$$

The Heaviside function enforces the required causality. Note that there are two possible time-orderings of the vertices that cancel the factor of $1/2$ from the second order expansion. The one-loop correction is a simple Gaus-

sian integral:

$$\delta\tilde{\Gamma}_1(t_2-t_1) = \lambda_0^2 \int \frac{d^dk}{(2\pi)^d} e^{-(D_A+D_B)k^2(t_2-t_1)} \tag{54}$$

$$= \frac{\lambda_0^2}{[4\pi(D_A+D_B)(t_2-t_1)]^{d/2}} \tag{55}$$

assuming $t_2 > t_1$. Clearly this depends only on $\tau = t_2 - t_1$, so it is natural to take a Laplace transform. Putting it together with the tree-level contribution, we find

$$\tilde{\Gamma}_{\text{one loop}}(s) = \lambda_0 - \frac{\lambda_0^2\Gamma(1-d/2)}{[4\pi(D_A+D_B)]^{d/2}} s^{d/2-1} + \mathcal{O}(\lambda_0^3) \tag{56}$$

which has the anticipated pole in the gamma function at $d_c = 2$.

Anticipating an epsilon expansion around $d_c = 2$, we write $\epsilon = 2 - d$ and define

$$I(s) = \frac{\Gamma(\epsilon/2)}{[4\pi(D_A+D_B)]^{1-\epsilon/2}} s^{-\epsilon/2} \tag{57}$$

With this notation, $\tilde{\Gamma}_{\text{one loop}}(s) = \lambda_0 - \lambda_0^2 I(s)$, and it is easy to see that the full renormalized vertex function consists simply of chaining arbitrarily many of these loop diagrams together. Schematically, we have

$\tilde{\Gamma} =$ 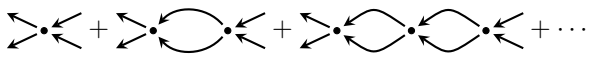 $+ \cdots$

This results in the exact geometric series

$$\tilde{\Gamma}(s) = \lambda_0 \sum_{n=0}^{\infty} (-\lambda_0 I(s))^n = \frac{\lambda_0}{1+\lambda_0 I(s)} \tag{58}$$

Thus the vertex function can be resummed to all orders. This simplification follows from the structure of the reaction vertices: each vertex contains one incoming a line and one incoming b line, so the only primitive vertex renormalization is generated by repeated A-B bubbles. There is no independent propagator renormalization unlike for, e.g., a ϕ^4 theory. Since $I(s) > 0$, the renormalized vertex function is clearly smaller than the bare vertex, indicating an effective screening of the reaction rate.

The Laplace variable s is an inverse time, so we can examine the behavior of the renormalized reaction rate in different limits. In the short-time limit $s \to \infty$, $I(s) \to 0$ so that $\tilde{\Gamma}$ is equal to its bare value, as we expect. In the long-time limit $s \to 0$ and $d > 2$, $I(s) \to$ constant (as defined by analytic continuation), representing a finite (but non-universal) renormalization of the reaction rate, as expected above the upper critical dimension. For $d < 2$, $I(s) \to \infty$, so that $\tilde{\Gamma} \to 0$, i.e. the reaction becomes completely diffusion-limited. At $d = 2$ we find the expected logarithmic decay of the reaction rate.

The bare reaction rate λ_0 is not dimensionless, and thus not a good expansion parameter for the subsequent renormalization group analysis. Thus we define the dimensionless bare coupling constant

$$g_0 = \frac{\lambda_0}{D_{\text{eff}}} \kappa^{-\epsilon} \tag{59}$$

where $D_{\text{eff}} = D_A + D_B$ and κ is the (arbitrary) initial momentum scale at which the theory is defined. The renormalized coupling is found by evaluating the resummed vertex function at zero external momenta and at the normalization point $s = D_{\text{eff}}\kappa^2$:

$$g_R = \left.\frac{\tilde{\Gamma}(s)}{D_{\text{eff}}} \kappa^{-\epsilon}\right|_{s=D_{\text{eff}}\kappa^2} \tag{60}$$

After some algebra, one finds

$$g_R = \frac{g_0}{1 + (4\pi)^{\epsilon/2-1}\Gamma(\epsilon/2) g_0} \equiv Z_g g_0 \tag{61}$$

where the multiplicative renormalization factor $Z_g^{-1} = 1 + g_0 B\Gamma(\epsilon/2)$ (defining $B = (4\pi)^{\epsilon/2-1}$) carries the pole $\Gamma(\epsilon/2) \sim 2/\epsilon$.

The next step is to find the beta function of the running coupling g_R. Concretely

$$\beta_g(g_R) \equiv \frac{dg_R}{d\ln\kappa} \tag{62}$$

$$= \kappa Z_g \frac{dg_0}{d\kappa} + \kappa g_0 \frac{dZ_g}{d\kappa} \tag{63}$$

$$= g_R \left(-\epsilon - \kappa \frac{d\ln Z_g^{-1}}{d\kappa} \right) \tag{64}$$

$$\beta_g(g_R) = 2g_R \left(-\frac{\epsilon}{2} + g_R B\Gamma\left(1+\frac{\epsilon}{2}\right) \right) \tag{65}$$

where we have written everything in terms of g_R and used $x\Gamma(x) = \Gamma(x+1)$. As Täuber et al. note, the exact quadratic form of the beta function is a simplification that can be traced back to the fact that the one-loop calculation explains the renormalization group analysis to all orders, which is not the case for typical theories.

Clearly, the beta function has only one non-trivial fixed point at which the theory is scale invariant:

$$g_R^* = \frac{1}{B\Gamma(\epsilon/2)} \sim \epsilon \tag{66}$$

Up to this point, the procedure for our reaction of interest ($A + B \to 0$) has been nearly identical to that for the simpler reaction $A + A \to 0$. However, in the following, we depart from Täuber et al.'s analysis to study the more complex reaction $A + B \to 0$. We assume that the initial condition satisfies $a_0 < b_0$ and employ the Callan-Symanzik equation to obtain the asymptotic behavior of the density $a(t)$. The key observation is that the density, written in terms of the renormalized parameters, appears to depend on the arbitrary momentum scale κ, but this is unphysical. The Callan-Symanzik equation encodes the requirement that the density not depend on

κ. A subtlety of the $A+B\to 0$ reaction is that the density of the minority species (here taken to be A) depends on the initial condition $\Delta \equiv b_0 - a_0 > 0$. Note that $\Delta(t) = b(t) - a(t) = \Delta$ is conserved because the reaction always removes one A and one B particle. Thus we have $a = a(t, a_0, \Delta, D_{\rm eff}, g_R, \kappa)$. The Callan-Symanzik equation reads

$$\frac{d}{d\ln\kappa} a(t, a_0, \Delta, D_{\rm eff}, g_R, \kappa) = 0 \tag{67}$$

Expanding the total derivative we find

$$\left[\kappa\frac{\partial}{\partial\kappa} + \beta_g(g_R)\frac{\partial}{\partial g_R}\right] a(t, a_0, \Delta, D_{\rm eff}, g_R, \kappa) = 0 \tag{68}$$

This appears to depend on five variables, but a dimensional analysis argument reduces the number of independent variables to four because we have

$$a(t, a_0, \Delta, D_{\rm eff}, g_R, \kappa) = \kappa^d \tilde{a}(t/t_0, a_0/\kappa^d, \Delta/\kappa^d, g_R) \tag{69}$$

where the timescale $t_0 = 1/D_{\rm eff}\kappa^2$ is defined at the normalization point. Computing all the partial derivatives with respect to κ and writing $a \equiv a(t, a_0, \Delta, D_{\rm eff}, g_R, \kappa)$, we find

$$\begin{aligned}\Big[2D_{\rm eff}t\frac{\partial}{\partial(D_{\rm eff}t)} - da_0\frac{\partial}{\partial a_0} - d\Delta\frac{\partial}{\partial\Delta} \\ + \beta_g(g_R)\frac{\partial}{\partial g_R} + d\Big]a = 0.\end{aligned} \tag{70}$$

The CS equation can be solved exactly by the method of characteristics, using the tree level (mean field) result

$$a_{\rm tree}(t) \sim a_0 e^{-\Delta\lambda_0 t} \tag{71}$$

as boundary data. The procedure is quite complicated, though standard, so we will not go into the details here. The result is that the running coupling flows to the IR fixed point g_R^* and, in this regime, the density decays asymptotically as

$$a(t) \sim a_0 \exp\left[-(\text{const.})\mathrm{g_R^*(D_{eff}t)^{d/2}}\right] \tag{72}$$

for $d < 2$, matching the stretched exponential form that Täuber et al. briefly quoted without justification. For $d > 2$, the reaction rate flows to a finite (non-universal) effective value, so the minority density decays as

$$a(t) \sim a_0 \exp[-\lambda_{\rm eff} t]$$

At $d = 2$, the marginal flow gives

$$a(t) \sim a_0 \exp[-(\text{const.})\mathrm{g_R^* D_{eff} t/\ln(D_{eff} t)}].$$

as quoted by Täuber et al.

For comparison, the simpler $A+A\to 0$ reaction, which has the tree-level result $a_{\rm tree}(t) \sim (\lambda_0 t)^{-1}$, becomes, after the RG analysis, $a(t) \sim t^{-d/2}$. We see that the RG result $t^{-d/2}$ is slower than mean field for $d < 2$ due to the corrections from density fluctuations. Above $d_c = 2$, the mean field result is correct and the RG analysis only contributes a non-universal amplitude correction.

B. $A+B\to 0$: A undergoing Lévy flights

Consider the same reaction $A+B\to 0$ but suppose A undergoes Lévy flights, such that it displays superdiffusive behavior. We argue that the RG procedure gives exactly the same results as above but with the replacements:

$$d_c = \sigma \tag{73}$$

$$\epsilon = \sigma - d \tag{74}$$

$$\to a(t) \sim a_0 \exp\left[-(\text{const.})g_\sigma^*(D_A t)^{d/\sigma}\right] \tag{75}$$

consistent with a modified upper critical dimension of $\sigma < 2$. (Note that the fixed point g_σ^* has also been modified). We justify this replacement in more detail below. First, however, it is interesting to note that this asymptotic result is identical to the result for both species undergoing Lévy flights, albeit with a different diffusion constant. Intuitively, A diffuses faster than B, so, on large length and time scales, B appears effectively stationary compared to A. The normal diffusion of B produces subleading corrections. This interpretation aligns with the more careful analysis that we now present.

As in the case of standard diffusion, only the reaction rate λ_0 is renormalized, as described by the vertex function. The one loop contribution to the vertex function is

$$\delta\tilde{\Gamma}_{\text{one loop}}(t) = (-\lambda_0)^2 \int \frac{d^dk}{(2\pi)^d} G_A(k,t) G_B(-k,t) \tag{76}$$

$$= (\lambda_0)^2 \int \frac{d^dk}{(2\pi)^d} e^{-D_A k^\sigma t - D_B k^2 t} \tag{77}$$

It is evident that the k^σ term dominates in the long time limit, so we can expand this integral to leading order in the small parameter $t^{1-2/\sigma}$. After some algebra, the result is

$$\begin{aligned}\delta\tilde{\Gamma}_{\text{one loop}}(t) = \frac{S_d}{(2\pi)^d\sigma}\Gamma\left(\frac{d}{\sigma}\right)(D_A t)^{-d/\sigma} \\ \times\left[1 - \frac{\Gamma\left(\frac{d+2}{\sigma}\right)}{\Gamma\left(\frac{d}{\sigma}\right)} D_B D_A^{-2/\sigma} t^{1-2/\sigma} + \cdots\right]\end{aligned} \tag{78}$$

After taking the Laplace transform and performing the exact vertex function resummation, the result is

$$\tilde{\Gamma}(s) = \frac{\lambda_0}{1 + \lambda_0 I(s)} \tag{79}$$

$$I(s) = I_0(s)\left[1 - D_B D_A^{-2/\sigma} C_{d,\sigma} s^{(2-\sigma)/\sigma} + \cdots\right] \tag{80}$$

$$I_0(s) = \frac{S_d}{(2\pi)^d\sigma} D_A^{-d/\sigma}\Gamma\left(\frac{d}{\sigma}\right)\Gamma\left(1 - \frac{d}{\sigma}\right) s^{d/\sigma - 1} \tag{81}$$

with $C_{d,\sigma} = \frac{\Gamma\left(\frac{d+2}{\sigma}\right)\Gamma\left(2 - \frac{d+2}{\sigma}\right)}{\Gamma\left(\frac{d}{\sigma}\right)\Gamma\left(1 - \frac{d}{\sigma}\right)}$. Clearly all corrections to $I(s)$ vanish in the long time ($s \to 0$) limit since $\sigma < 2$. By

comparing to the presentation following the calculation of the renormalized vertex function in the previous section, we see that our previous results with the replacements $d_c = \sigma$ and $\epsilon = \sigma - d$ are asymptotically exact for A undergoing Lévy flights, giving

$$a(t) \sim a_0 \exp\left[-(\text{const.}) g_\sigma^* (D_A t)^{d/\sigma}\right] \tag{82}$$

Combining the results from mean field theory in Sec. III, we can summarize the scalings for all cases in the two tables below, where c is a constant:

	$d < 2$	$d \geq 2$
$a_0 = b_0$	$(Dt)^{-d/4}$	
$a_0 < b_0$	$\exp\left[-c(Dt)^{d/2}\right]$	$e^{-\lambda_0 t}$

Table I: Scaling of $a(t)$ with standard diffusion.

	$d < \sigma$	$d \geq \sigma$
$a_0 = b_0$	$(Dt)^{-d/2\sigma}$	
$a_0 < b_0$	$\exp\left[-c(Dt)^{d/\sigma}\right]$	$e^{-\lambda_0 t}$

Table II: Scaling of $a(t)$ with Lévy flights on A.

Note that we do not consider any logarithmic corrections exactly at the upper critical dimension.

We can further generalize to the case that A and B both undergo Lévy flights, perhaps with different exponents. Consider the case $0 < \sigma_A < \sigma_B < 2$. Then it is clear from the above analysis that the asymptotic behavior will be determined by the smaller of the two exponents, in this case σ_A, with the importance of the correction from the diffusion of B determined by the difference $\sigma_B - \sigma_A$. Thus we have treated the most general possible set of diffusion conditions for the reaction $A + B \to 0$.

V. NUMERICAL SIMULATIONS

We first consider the $A + B \to 0$ process on a lattice with standard diffusion, random initial conditions, and average densities ρ_A and ρ_B. This is a Markov process: a particle of species A (B) can make nearest-neighbor hops at a rate $1/D_A$ ($1/D_B$). Each particle has $z = 2d$ nearest neighbors, and each of the N_A (N_B) particles is independent.

To numerically simulate this process, we use the Gillespie algorithm [14]:

1. For each site, sample from Poisson(ρ_A) and Poisson(ρ_B) to determine the number of A and B particles, respectively. Immediately annihilate any A–B pairs on the same site so that only a single species is present on a given site.

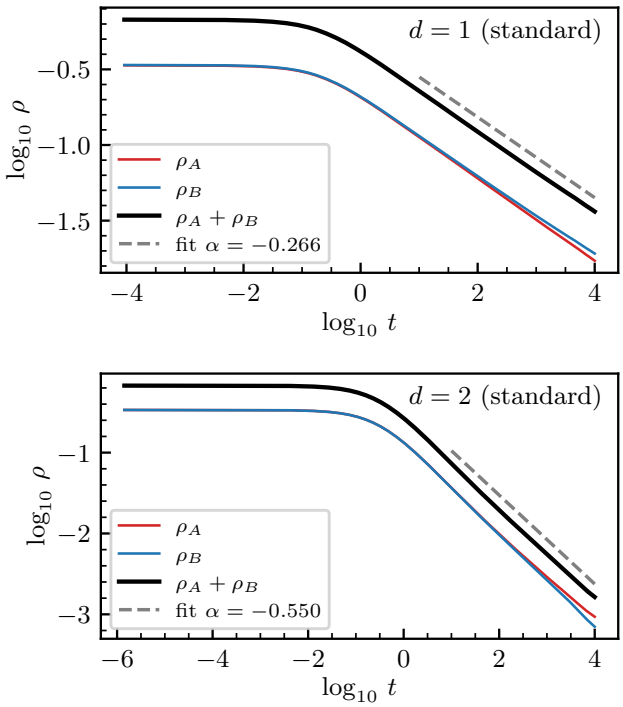

FIG. 1. Ensemble-averaged particle density for the $A+B \to 0$ reaction with standard diffusion and equal densities ($\rho_A = \rho_B = 0.5$, Poisson-distributed) and periodic boundary conditions. Results are averaged over 100 independent realizations. (Top) $d = 1$: linear lattice of $L = 8192$ sites, run to $t = 10^4$. (Bottom) $d = 2$: square lattice of 512×512 sites, run to $t = 10^4$. In each panel, ρ_A (red) and ρ_B (blue) are shown separately; their sum (black) is fit over the final three decades (dashed gray). The fit exponents are $\alpha = -0.266$ for $d = 1$ and $\alpha = -0.550$ for $d = 2$, in agreement with the theoretical decay $\alpha = -d/4$.

2. Randomly select species A or B weighted by total rates of each: $\omega_A = 1/2dN_A D_A$, $\omega_B = 1/2dN_B D_B$, and $\mathbb{P}(A \text{ selected}) = \omega_A/(\omega_A + \omega_B)$.

3. Uniformly pick a random particle of the selected species.

4. Uniformly pick a random hop direction.

5. Move the particle.

6. If there is an opposite-species particle present at the destination, annihilate the particles immediately. This is the limit of infinite reaction rate.

7. Step time: $\Delta t = 1/(\omega_A + \omega_B)$.

8. Repeat Steps 2–7 until the desired time is reached.

We run this simulation for equal densities $\rho_A = \rho_B = 0.5$ for both $d = 1$ and $d = 2$ with periodic boundary conditions and show the decay of the densities in Fig. 1. To save memory, we avoid saving the particle locations of

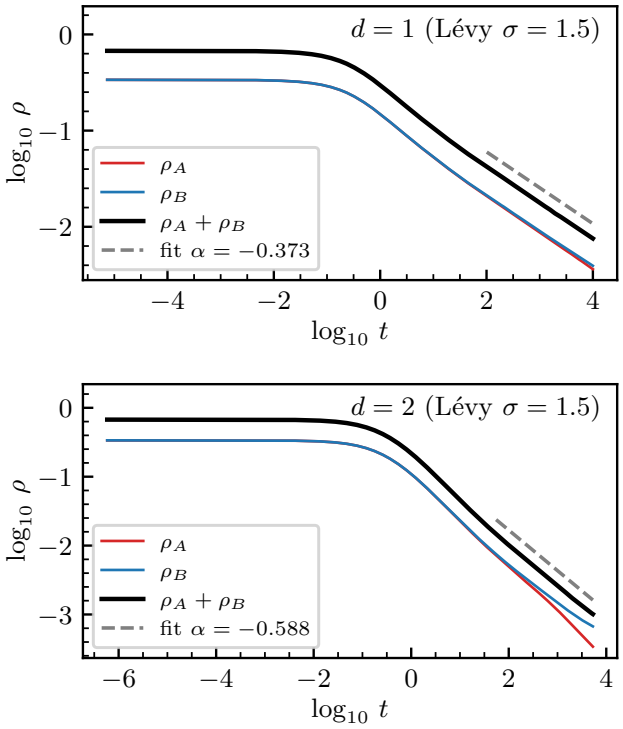

FIG. 2. Particle density for the $A + B \to 0$ reaction with Lévy flights ($\sigma = 1.5$) for both species, ensemble-averaged over 10 runs for $d = 1$ ($L = 262144$) and $d = 2$ ($L = 1024$). An empirical fit to the last two decades gives a fit exponent $\alpha = -0.373$ for $d = 1$ and $\alpha = -0.588$ for $d = 2$, in rough agreement with $\alpha = -d/2\sigma$.

the simulation at every time step; rather, we take snapshots at 500 log-spaced frames. Because the Poisson-distributed particle number does not generally give equal particle numbers for A and B in the finite simulation, there are small differences in the densities ρ_A and ρ_B that are exemplified at late times. To reduce this effect, we run an ensemble with 100 simulations starting from different random initial conditions. We also measure the power law scaling against $\rho_A + \rho_B$, which scales like the individual densities but is more robust to these small variations. We recover the standard result $\rho \sim t^{-d/4}$ for equal densities.

To incorporate Lévy flights into the simulation, we must be careful. Particles can now jump arbitrarily far instead of just to their nearest neighbors. A randomly selected nearest neighbor is now replaced with a uniformly selected hop direction and a step length sampled from $r \sim \text{Pareto}(1, d + \sigma - 1)$ where the probability density function of $\text{Pareto}(r_m, \alpha)$ is

$$f(r; r_m, \alpha) = \begin{cases} \alpha r_m^\alpha / r^{\alpha+1} & r \geq r_m \\ 0 & r < r_m. \end{cases} \tag{83}$$

This Pareto distribution has a power-law tail with $f(r; r_m, \alpha) \sim 1/r^{d+\sigma}$ that characterizes Lévy flights.

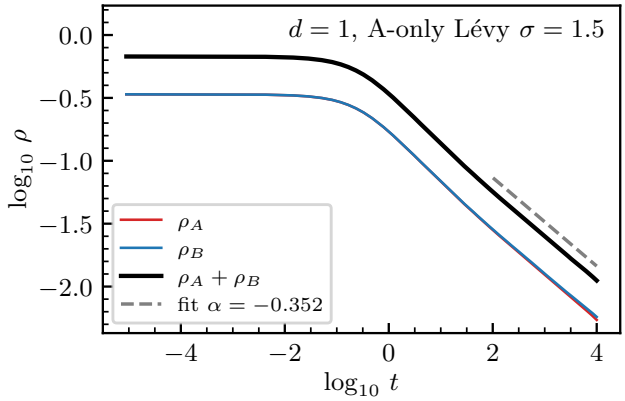

FIG. 3. The $A + B \to 0$ reaction with only species A performing Lévy flights ($\sigma = 1.5$) while species B has standard diffusion, with the same ensemble numerical parameters as Fig. 2 for $d = 1$. A fit exponent $\alpha = -0.352$ demonstrates that the superdiffusion of A dominates.

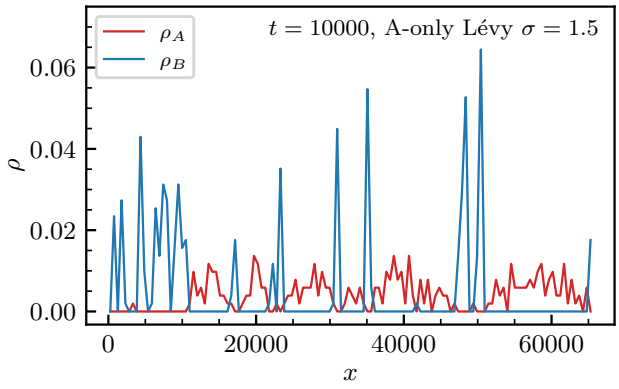

FIG. 4. Snapshot of the density profiles ρ_A (red) and ρ_B (blue) at the final time ($t = 10^4$) for one A-only Lévy simulation (Fig. 3). The local density is computed using 128 bins across the domain. There is clear asymmetry between the A and B regions.

Once a displacement vector is drawn, the nearest lattice site is the selected hop site. With periodic boundary conditions, hops may span the entire domain size or more; these hops are accounted for. In fact, it is important that we do not cut off the distribution because the infinite variance of the distribution must be retained. Note that we do not pick a random axis-aligned direction as we do in the standard case. This is allowed in the standard case because axis-aligned Gaussian steps produce isotropy ($e^{-x^2}e^{-y^2} = e^{-r^2}$) but axis-aligned Lévy flights do not ($x^{-d-\sigma}y^{-d-\sigma} \neq r^{-d-\sigma}$).

Although this distribution sets the relative rates between different hops, we have freedom to select a reference rate. We set the normalization so that the nearest-neighbor hops have the same rate as before of $1/D_A$ ($1/D_B$). However, the diffusion constant is now dimen-

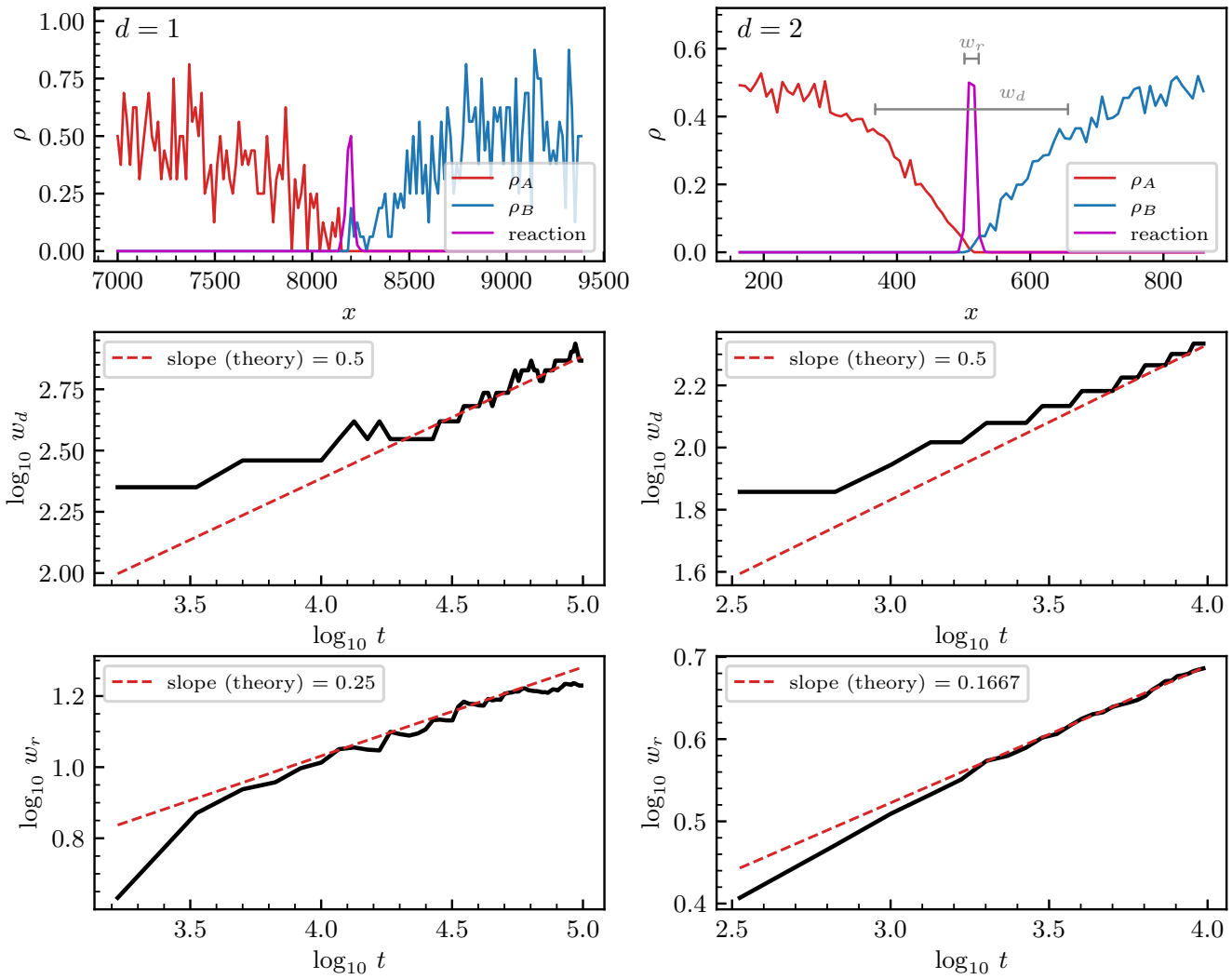

FIG. 5. The $A + B \to 0$ process in $d = 1$ and $d = 2$ with standard diffusion and segregated initial conditions: A starts on the left half of the domain and B starts on the right half. (Top) Spatial density profiles near the reaction front at $t = 10^5$ ($d = 1$, $L = 16384$) and $t = 10^4$ ($d = 2$, $L_x \times L_y = 1024 \times 64$). The reaction zone (magenta, rescaled for visualization) is the region where reactions have occurred: it is the accumulation of inert product C in the $A + B \to C$ reaction. The reaction zone (w_r) is embedded in the depletion zone (w_d) in which A and B are depleted. (Middle) Depletion zone width $w_d(t)$ on a log-log scale measured by the region in which $< 85\%$ of the initial density remains; the dashed red line verifies the theoretical prediction $w_d \sim t^{1/2}$. (Bottom) Reaction zone width $w_r(t)$ on a log-log scale measured by the standard deviation of the inert product distribution; the dashed red line shows $w_r \sim t^{1/4}$ ($d = 1$) and $w_r \sim t^{1/6}$ ($d = 2$), in agreement with Lee–Cardy theory [15].

sionally different than the standard case, so this is a rather arbitrary choice. Because we are seeking universal properties, we do not expect this to affect the results significantly.

In Fig. 2, we show the results of simulations with Lévy flights where both species A and B have equal densities. In light of the discussion in Sec. IV, we enable Lévy flights for both species with $\sigma = 1.5$, and we claim that this has the same scaling as the regime with Lévy flights restricted to A. We find rough agreement with the scaling law $\rho \sim t^{-d/2\sigma}$, with better agreement for $d = 1$. These simulations are more intensive than comparable standard simulations because the long-range hops cause more reactions and can lead to worse finite-size effects. We suspect this contributes to the deviation for $d = 2$, which we were only simulate on a 1024×1024 grid.

In Fig. 3, we verify the above claim by only turning on Lévy flights for species A and find that the density scaling is quite similar. This is the expected behavior: the superdiffusion of A dominates. However, this does not mean the asymmetric case is identical to the symmetric case. In Fig. 4, we show the late-time density profiles for an asymmetric simulation. We find that the A domains are less dense and span larger length scales

compared to the B domains. Physically, this is not surprising; however, it would be interesting to determine more quantitative properties of these domains.

Ideally, we would like to demonstrate the corrections to scaling for the *unequal density* regimes as shown in Sec. IV. However, these regimes are particularly hard to probe numerically. Exponential decays are generally hard to measure with discrete particles: many particles still need to be present after initial transient effects and before discretization effects to fit an exponential decay for sufficient time. Fitting a stretched exponential—that is, fitting a power law to the logarithm of the density—is even more difficult. Specialized numerical techniques requiring hundreds of hours of CPU time are necessary [16], and even these techniques produce large deviations from theory.

However, with our current simulations, we can still observe scaling changes below the upper critical dimension with *segregated* initial conditions: placing all A on one side of the domain and all B on the other. In standard diffusion, reactions can only occur near the interface: this produces a *reaction zone* where reactions occur and a *depletion zone* where A and B particles are depleted: see the top subplots in Fig. 5. The reaction and depletion zones are characterized by widths w_r and w_d, respectively. Lee and Cardy [15] found that, for standard diffusion,

$$w_r \sim \begin{cases} t^{\frac{1}{2(d+1)}} & d \leq 2 \\ t^{1/6} & d > 2, \end{cases} \tag{84}$$

$$w_d \sim t^{1/2}. \tag{85}$$

In particular, the reaction zone power law changes at the upper critical dimension $d_c = 2$. In Fig. 5, we confirm these scalings. The two species are initialized on separate sides of the domain, and hard-wall boundary conditions are enforced on the axis orthogonal to the interface.

In Fig. 6, we repeat the analysis of the reaction zone and depletion zone in $d = 1$ with both species exhibiting Lévy flights with $\sigma = 1.5$. We find that both scaling laws change. This is not surprising since the particles can now hop further. We currently do not have supporting theory or 2D simulations, but this suggests a promising direction for using simulations to probe changes at and below the upper critical dimension $d_c = \sigma$.

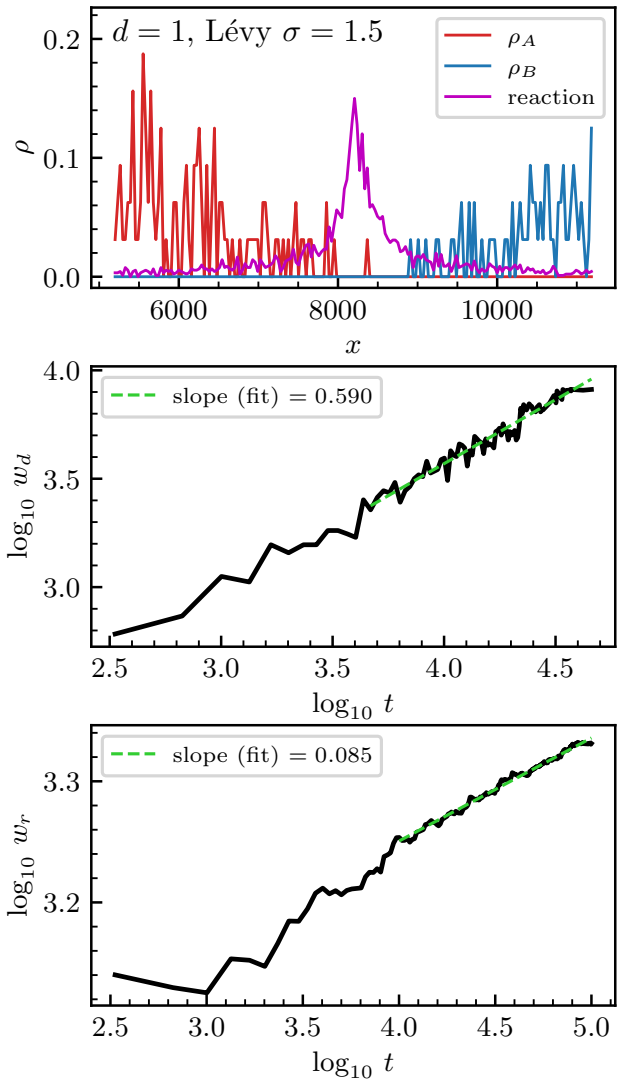

FIG. 6. The segregated $A + B \to 0$ process in $d = 1$ in which both species perform Lévy flights ($\sigma = 1.5$, $d = 1$). The depletion zone width $w_d(t)$ and reaction zone width $w_r(t)$ are fit (green) to the last decade for empirical power law scalings that deviate from the standard diffusion case (see Fig. 5).

VI. DISCUSSION

In this paper, we applied field theoretic and renormalization group methods to study the chemical reaction $A+B \to 0$ under various conditions. First, we derived the Doi-Peliti field theory from the master equation. We then used the renormalization group to obtain the asymptotic statistics of the reaction under normal diffusion and long-ranged Lévy flights. We validated our results with numerical simulations and studied other phenomena including the scaling of the depletion layer between segregated reactant domains.

This work leaves several avenues open for future research. In the case of the depletion zone, we assumed A and B both underwent the same diffusive behavior: both standard and both Lévy. If only one species underwent Lévy flights, presumably the reaction and depletion zone would form a traveling wave. It would be interesting to calculate the speed of the front as a function of σ. Numerically, we would like to run larger simulations that reduce finite size effects; the higher dimension and unequal density cases are particularly challenging.

Finally, future work should investigate more biologically realistic models. In particular, Lévy flights allow

for arbitrarily large jumps in the same fixed time at each step. A more realistic model may involve Lévy *walks* in which particles move at a finite velocity for a variable time between each step, like run-and-tumble particles [3].

ACKNOWLEDGMENTS

We thank Prof. Mehran Kardar for a great semester, and we thank Prof. Sunghan Ro for valuable discussions.

CONTRIBUTIONS

Adele Basturk performed the calculations for Doi-Peliti field theory and wrote the corresponding section. Nicholas Lawson performed the RG analysis and wrote the corresponding section. Troy Tsubota performed the mean field theory, carried out the numerical simulations, and wrote the corresponding sections. All authors contributed to conceptualization, writing, and editing.

[1] U. C. Täuber, M. Howard, and B. P. Vollmayr-Lee, Applications of field-theoretic renormalization group methods to reaction–diffusion problems, Journal of Physics A: Mathematical and General **38**, R79 (2005).

[2] G. M. Viswanathan, ed., *The Physics of Foraging: An Introduction to Random Searches and Biological Encounters* (Cambridge University Press, Cambridge New York, 2011).

[3] O. Bénichou, C. Loverdo, M. Moreau, and R. Voituriez, Intermittent search strategies, Reviews of Modern Physics **83**, 81 (2011).

[4] T. H. Harris, E. J. Banigan, D. A. Christian, C. Konradt, E. D. Tait Wojno, K. Norose, E. H. Wilson, B. John, W. Weninger, A. D. Luster, A. J. Liu, and C. A. Hunter, Generalized Lévy walks and the role of chemokines in migration of effector CD8+ T cells, Nature **486**, 545 (2012).

[5] D. C. Vernon, Long range hops and the pair annihilation reaction A + A $\rightarrow$ 0 : Renormalization group and simulation, Physical Review E **68**, 041103 (2003).

[6] B. P. Lee and J. Cardy, Renormalization group study of theA+B$\rightarrow \oslash$ diffusion-limited reaction, Journal of Statistical Physics **80**, 971 (1995).

[7] U. C. Täuber, *Critical Dynamics: A Field Theory Approach to Equilibrium and Non-Equilibrium Scaling Behavior* (Cambridge University Press, Cambridge, 2014).

[8] D. Shapoval, V. Blavatska, and M. Dudka, Survival in two-species reaction-diffusion system with Lévy flights: Renormalization group treatment and numerical simulations, Journal of Physics A: Mathematical and Theoretical **55**, 455002 (2022).

[9] Š. Birnšteinová, M. Hnatič, and T. Lučivjanský, Two-Species Reaction-Diffusion System: The Effect of Long-Range Spreading, EPJ Web of Conferences **226**, 02005 (2020).

[10] M. Hnatič, M. Kecer, and T. Lučivjanský, Renormalization Group Analysis of Two-Species Reaction-Diffusion System: Crossover between Long-Range and Short-Range Spreading, Physics of Particles and Nuclei Letters **22**, 522 (2025).

[11] M. Doi, Second quantization representation for classical many-particle system, Journal of Physics A: Mathematical and General **9**, 1465 (1976).

[12] L. Peliti, Path integral approach to birth-death processes on a lattice, Journal de Physique **46**, 1469 (1985).

[13] A. lefevre and G. Biroli, Dynamics of interacting particle systems: Stochastic process and field theory, Journal of Statistical Mechanics: Theory and Experiment **2007**, P07024 (2007), arXiv:0709.1325 [cond-mat.stat-mech].

[14] D. T. Gillespie, Stochastic Simulation of Chemical Kinetics, Annual Review of Physical Chemistry **58**, 35 (2007).

[15] B. P. Lee and J. Cardy, Scaling of reaction zones in the $A + B \rightarrow 0$ diffusion-limited reaction, Physical Review E **50**, R3287 (1994).

[16] V. Mehra and P. Grassberger, Trapping reaction with mobile traps, Physical Review E **65**, 050101 (2002).